JACS
JOURNAL OF THE AMERICAN CHEMICAL SOCIETY

Article

pubs.acs.org/JACS

Self-Assembling Molecular Capsules Based on α,γ-Cyclic Peptides

Haxel Lionel Ozores, Manuel Amorín, and Juan R. Granja*

Centro Singular de Investigación en Química Biolóxica e Materiais Moleculares (CIQUS), and Departamento de Química Orgánica, Universidade de Santiago de Compostela, Santiago de Compostela 15782, Spain

Supporting Information

ABSTRACT: A new capsule based on a β-sheet self-assembling cyclic peptide with the ability to recognize and release several guests is described. The host structure is composed of two self-complementary α,γ-cyclic peptides bearing a Zn porphyrin cap that is used for the selective recognition of the guest. The two components are linked through two dynamic covalent bonds. The combination of binding forces, including hydrogen bonding, metal coordination, and dynamic hydrazone bonds, allows the reversible recognition of long bipyridine guests. The affinity for these ligands showed a strong dependence on the guest length. Delivery of the encapsulated ligand can be achieved by hydrolysis of hydrazones to disrupt the sandwich complex structure.

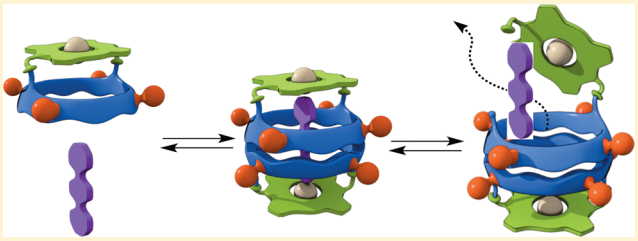

INTRODUCTION

The emergence of nanometric-sized molecular capsules has revolutionized chemistry, nanotechnology, and materials science.[1] These molecular containers are empty structures generated by the self-assembly of small components. The stimulating novel aspect of these structures is their inner space, which shows unique properties that differ from the bulk solution.[2] As a result, these nanocapsules are considered as new and useful nanotechnological tools in different fields.[3] The original cages were covalently bound structures, such as the carcerands and hemicarcerands developed by Cram,[4] although the supramolecular variants were developed soon after. For that purpose Rebek and de Mendoza exploited the formation of several hydrogen bonds between two bis-glycoluril derivatives to create the tennis-ball supramolecular capsules.[5] Other authors subsequently used coordination chemistry to link an increased number of subunits to generate molecular filled capsules.[6] Molecular containers with large inner volumes have been developed using this approach.[7] Various applications have been proposed for these materials, and they include nanoreactors for catalysis and stabilization of reactive intermediates or labile chemical species, the emergence of novel stereoisomerisms, separation, and delivery and transport processes.[8,9] In general, the ensemble generates an empty inner volume that can be filled with appropriate guests. The strategies for the assembly of supramolecular capsules mainly employ hydrogen bonding, metal coordination, and hydrophobic interactions.[1,4] Most of these containers entrap the guest by complementary shape, and only a few examples incorporate appropriate functional groups to recognize specific ligands to enhance the molecular selection.[7,8c] In most cases, metals are simply structural components used to stabilize the capsule, and they do not play any role in the molecular recognition of the guest.

Metalloporphyrins have been widely employed as useful supramolecular tools to develop tweezers, nanorotors, receptors, and other hosts.[10] These kinds of structures are attractive because they can encode 180° or 90° angles and thus perform as ditopic units. Additionally, substitution of the metalloporphyrinic core allows the construction of tetratopic tectons. However, despite these properties, only a few examples of porphyrin-based self-assembling capsules have been reported in which the porphyrin components are not covalently attached and the guest is totally enclosed by the receptor.[11]

Over the past few years we have been working with self-assembling cyclic peptides (CPs) to form hollow structures such as nanotubes or toroids.[12] These structures share important features such as the potential modification of the external properties by changing the amino acid composition of the CP. The toroidal structures are open-ended assemblies formed by two CPs in which the amide protons of one of the disc-shaped faces are substituted by alkyl groups.[13] The inclusion of γ-amino acids provided CPs with larger association constants and tunable internal properties.[13a−c,14] We anticipated that the incorporation of a stopper at each end of the dimer may provide empty spaces that could be used in the encapsulation of different guests (Scheme 1).[15]

On the basis of the assumption outlined above, we present a new molecular capsule with a large cavity size. The preparation, assembly, and recognition processes of this novel capsule combine different supramolecular strategies, including hydrogen bonding to open/close the capsule, metal coordination for ligand recognition, and dynamic covalent bonds for the synthesis of molecular components and ligand delivery.

RESULTS

Design. The cyclic octapeptide template has alternating α-amino acids and non-natural *N*-methylated 3-aminocyclopenta-

Received: October 5, 2016
Published: December 20, 2016

DOI: 10.1021/jacs.6b10456
J. Am. Chem. Soc. 2017, 139, 776−784

Scheme 1. Proposed Model for Capsule Design Using Cyclic Peptide Components[a]

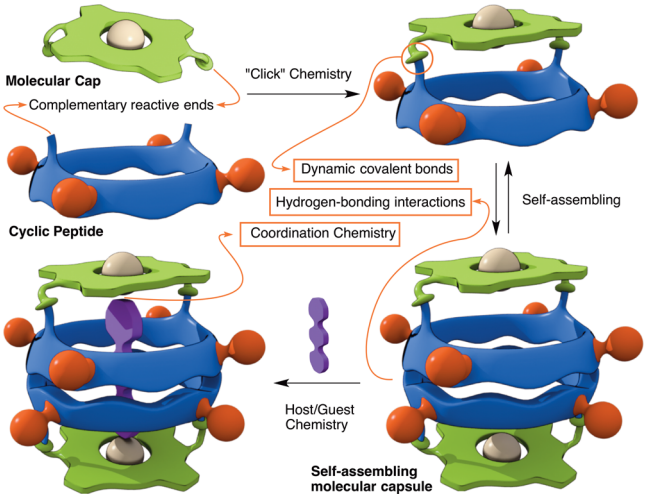

[a]The use of complementary reactive ends in the cyclic peptide and the molecular cap would facilitate the formation of the self-assembling capsule.

necarboxylic acids (γ-^{Me}*N*-Acp).[13,16] The C_4 symmetry of the octapeptide allows the incorporation of only two reactive anchors, and this generates capsules with C_2 symmetry, *vide infra*. The metalloporphyrin caps were selected due to the previously mentioned structural properties and the complementary symmetry (C_4/C_2) with cyclic octapeptides.[10,17] In addition, the porphyrinic metal core could direct the encapsulation of specific ligands toward the capsule cavity. In order to attach the molecular cap we decided to replace some of the methyl groups for a functionalized spacer. We envisaged the use of a covalent reversible hydrazone to connect the two components. This process links the two parts in a dynamic and reversible manner, and this provides an additional level of control of the capsule. Under these premises, the syntheses of porphyrin **1** and cyclic peptide **CP1** were proposed using the synthetic strategy shown in Scheme 2.

Porphyrin **1** could be prepared by MacDonald-type 2 + 2 condensation using the sterically hindered 5-dipyrromethane **2** with *meta*-formyl-protected benzaldehyde **3**.[18] The carbonyl group was placed at the *meta*-position to facilitate the attachment of the cyclic peptide. The cyclic peptide (**CP1**) would bear the hydrazide moieties to be incorporated at the peptide backbone through a Fukuyama sulfonamide alkylation of nosylate **7**.[19] The γ-amino acid (1*R*,3*S*)-Acp was alternated with natural D-leucine. The synthesis would be carried out in solution phase using the previously reported convergent approaches.[13] In this case we developed a modified strategy in which benzyl carbamate and methyl ester groups were used to protect the amino and carboxylic acid groups, respectively. This combination allowed the use of *tert*-butyl groups (ester and carbamate) for the protection of the anchor groups, thus avoiding complications during deprotection of the carboxylic acid group under basic conditions.[20]

Synthesis of Capsule CP3. Synthetic details for the preparation of porphyrin **1** and cyclic peptide **CP1** are illustrated in Schemes 1SI and 2SI in the Supporting Information. The condensation of Zn-porphyrin **9** with **CP1** was achieved by stirring a dilute solution of the two components in dichloromethane (Scheme 3). The resulting

Scheme 2. Retrosynthetic Analysis for the Synthesis of the Components of the Capsule

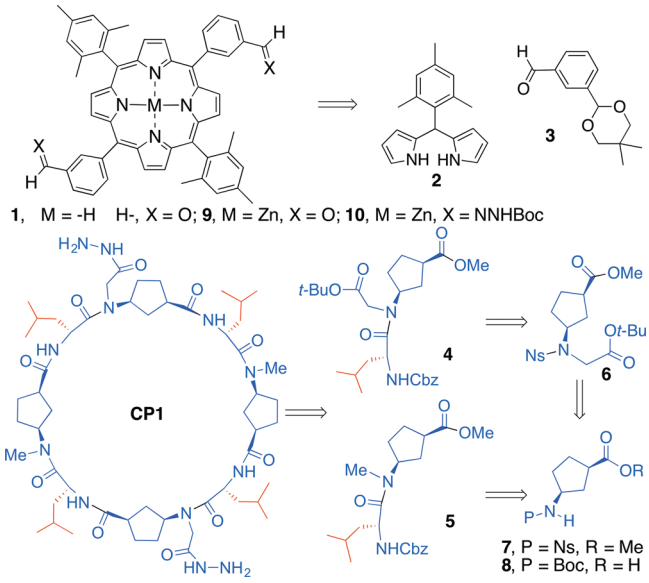

half-capsule **CP3**, the self-assembly process of which generates dimeric container **D3**, was obtained in 62% yield without loss of the zinc ion.

Scheme 3. Preparation of Cyclic Peptide-Porphyrin Hybrid (CP3) and Its Self-Assembling Process[a]

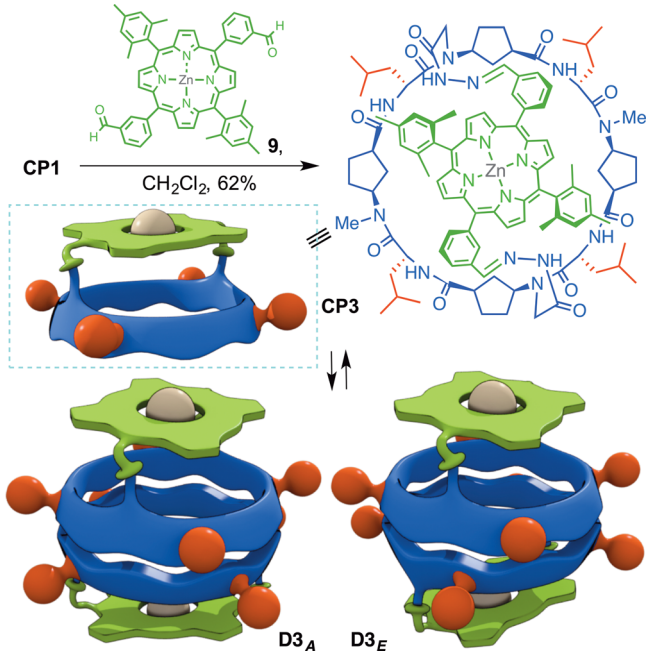

[a]Two different assemblies, the alternated ($\mathbf{D3}_A$) and the eclipsed ($\mathbf{D3}_E$) forms, can be formed depending on the relative amino acid pairwise arrangement.

Encapsulation Experiments. The encapsulation studies began with the design of a series of 4,4′-bipyridine ligands (Scheme 4). The ligands differ in length and the properties of the connectors between the two pyridine moieties. The lengths of the bipyridine ligands range from 12.3 to 21.2 Å considering the N-to-N distances. The synthetic strategies used for the

DOI: 10.1021/jacs.6b10456
J. Am. Chem. Soc. 2017, 139, 776−784

Scheme 4. Different Ligands (L*n*) Used in the Encapsulation Process and Binding Model with 10

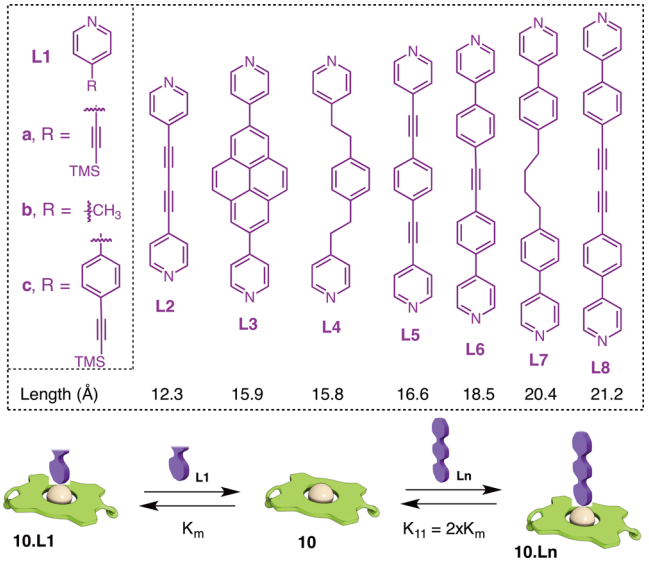

preparation of these ligands are shown in Scheme 3SI (Supporting Information).

Pyridine models **L1a–c** were used to estimate the affinity of pyridine moieties for zinc porphyrins in order to calculate the improvement in binding between the host (peptide capsule) and the bidentate ligands when they coordinate both zinc ions. The coordination of ligands was initially studied by UV–vis titrations in chloroform solution at constant host concentration.

The binding studies (Scheme 4) were started with model porphyrin **10**, which was obtained from **9** by treatment with Boc-protected hydrazine (Scheme 1SI). The association constants for model ligands and this porphyrin provided the affinity values reported in Table 1. The association constants were adjusted using the DynaFit[21,22] program considering a binding model that involved a stoichiometric state of the porphyrin **10** and the ligand. Affinity constants for ligands **L1a–c**, **L2**, **L3**, and **L5** with **10** are consistent with the preliminary results,[23] see Table 1 and Figure 1SI. The observed differences between diverse **L1** ligands confirmed the expected larger association constant for the most electron-rich ligand (picoline, **L1b**). The binding of bipyridine ligands (**L2**, **L3**, and **L5**) is reasonably consistent with the consideration of the pyridine concentration for these compounds at an identical concentration (for instance, [**L1a**] = [**L2**]), which is twice as high as in **L1**. The small differences observed suggest that the conjugation of these moieties might reduce the affinity of the pyridine moiety for the Zn-porphyrin complex. Despite this difference, we will consider the association constants of pyridines as reference models for zinc pyridine coordination.

The UV–vis spectra obtained during the titration of capsule **D3** with ligands were followed by the appearance of the Soret absorption band (at 431 nm) of the porphyrin, which is characteristic of an axially coordinated ligand (Figure 1). Exciton coupling between the porphyrin transitions was not observed in either the free ligand receptor or upon sandwich formation,[24] probably as a consequence of the long distance between the two porphyrins in receptor **D3**.

UV–vis measurements on capsule **D3** provided similar values for pyridine ligands (Figure 2SI), albeit 1 order of magnitude smaller. The values obtained for **L2** (Scheme 4), which were similar to those for **L1a** (Table 1), suggest that this ligand is too short, as one would expect, to extend across the cavity length, and therefore, it cannot simultaneously coordinate both zinc ions. The coordination probably takes place mainly at the outer face of the porphyrin moiety. In fact, the association constant calculated (2.4×10^6 M^{-2}) for the formation of aggregate **D3·2L2** (Scheme 5SI) is similar to that obtained for **L1a** (Table 1).

Next we considered rigid and longer ligands **L3** and **L5** (Scheme 4), which differ in their length at 15.9 and 16.6 Å, respectively. Both ligands have a similar association constant to **L2** with porphyrin **10** (Table 1). To our surprise, the UV–vis studies carried out with freshly prepared samples gave results that were not markedly different. It was necessary to add around 2000 equiv of **L3** to shift the equilibrium completely toward the porphyrin complex with the axially coordinated ligand (431 nm band). The measurements were repeated on the same samples after standing at room temperature for more than 5 h. In these new experiments the spectra changed and were consistent with a higher concentration of coordinated complex. In fact, it was only necessary to add less than 100 equiv of **L3** to observe exclusively the 431 nm band, see Figure 2SIe in the Supporting Information. This observation might suggest that the encapsulation is a slow process that requires several hours to reach equilibrium.[25] This result must be due to the need to disassemble the capsule in order for the ligand to be

Table 1

ligand (L*n*)	K_m(L*n*)[a] (M^{-1})	K_D(L*n*)[b] (M^{-2})	K(L*n*⊂D_3)[c] (M^{-1})	EM (M)	length (Å)
L1a	5.9×10^3	9.9×10^5			
L1b	1.7×10^4	2.6×10^7			
L1c	1.1×10^4	4.6×10^6			
L2	9.0×10^3	2.4×10^6[d]	1.1×10^3	2.7×10^{-4}	12.3
L3	1.8×10^4		1.1×10^5	6.0×10^{-3}	15.9
L4			1.2×10^8	1.1	15.8
L5	1.0×10^4		7.6×10^6	1.9	16.6
L6			1.8×10^6	9.9×10^{-2}	18.5
L7			6.2×10^5	3.4×10^{-2}	20.4
L8			6.2×10^4	3.4×10^{-3}	21.2

[a]The association constant was calculated using model porphyrin **10** (2 μM in $CHCl_3$) in a 1:1 binding model. [b]The association constant was calculated using model **D3** + 2**L1** ⇄ **D3·2L1**. [c]titrations were carried out at a constant concentration of **CP3** in chloroform (~0.5 μM for bipyridine ligands) using equilibrium model **D3** + L*n* ⇄ L*n*⊂**D3**. [d]The association constant was determined using the pyridine binding model (**D3** + 2 **L2** ⇄ **D3·2L2**).

DOI: 10.1021/jacs.6b10456
J. Am. Chem. Soc. 2017, 139, 776–784

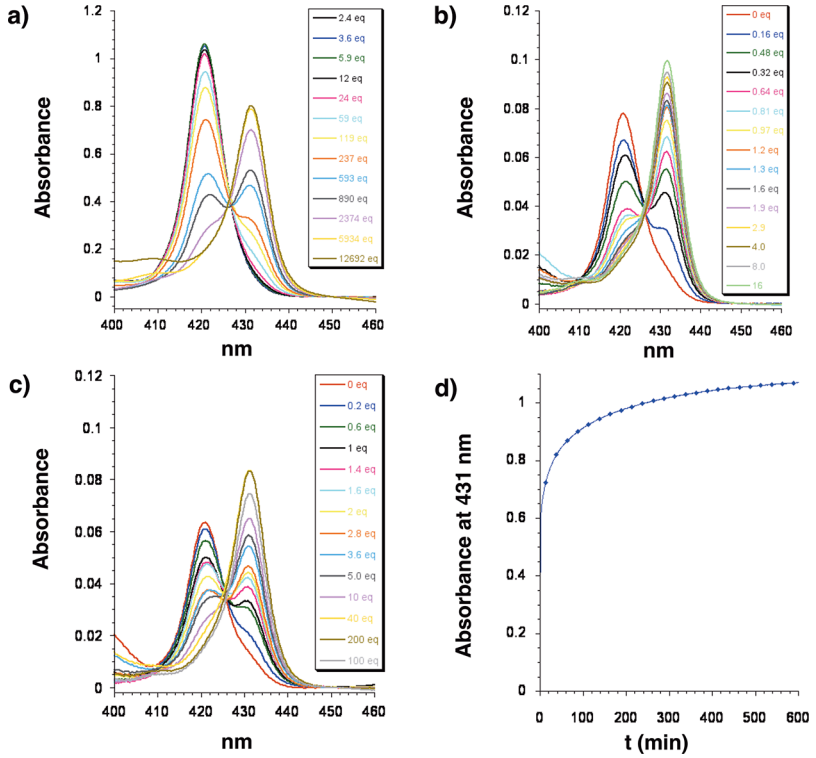

Figure 1. Selected spectra showing the Soret band region for the UV−vis titrations of **D3** with ligands (a) **L1a**, (b) **L4**, and (c) **L5**. The number of equivalents added is indicated in the inset. (d) Kinetic studies on the encapsulation process following the appearance of the 431 nm band with time after mixing capsule **D3** and **L5** in a 1:2 ratio.

able to reach the peptide internal cavity, see the Scheme 5 for the proposed biding model. Most probably **D3** can only

Scheme 5. Encapsulation Equilibria for Ligand Recognition

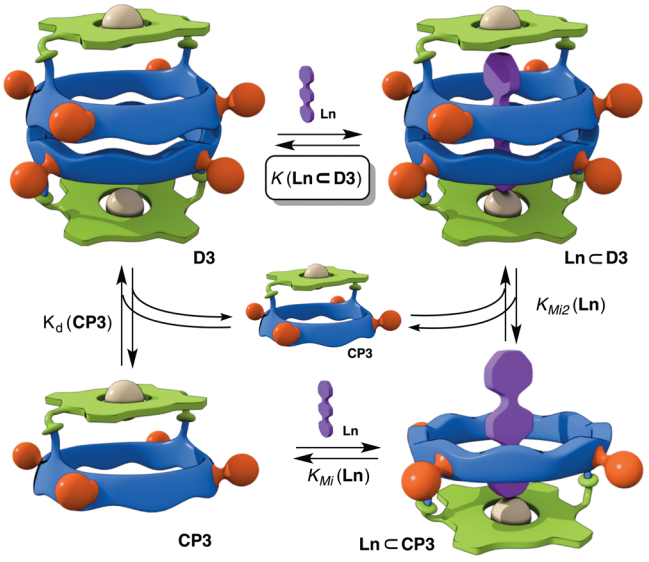

coordinate the ligands by the porphyrin external face to form empty dimers **D3·L*n*** and/or **D3·2L*n*** (Scheme 4SI). The concentration of the reactive monomeric form **CP3** is low considering the previously estimated association constant and the initial peptide concentration (2 μM).[26] This monomer can interact with the ligand through the internal or external porphyrin face to generate **CP3·L*n*** (Scheme 5SI) or **L*n*⊂CP3** (Scheme 5), respectively. Once the cavitand interacts with the ligand to form the **L*n*⊂CP3** complex, if the ligand has the appropriate size, the interaction with a ligand free CP must be very fast and favorable to form the encapsulated complex **L*n*⊂D3**.

In order to verify the rate of formation of **L5⊂D3**, kinetic experiments were carried out in which 2 equiv of **L5** were mixed with **D3**, and the appearance of the UV band at 431 nm was followed for 12 h, with data taken every 30 s (Figure 1d). The encapsulation process for **CP3** at a 2 μM concentration took more than 5 h to reach equilibrium. A similar result was obtained with ligand **L3** (Figure 3SI), and this confirms that the rate limiting step must be independent of ligand affinity.

Given the behavior outlined above, for encapsulation studies the solution mixtures were prepared 12 h in advance. Under these conditions, both ligands (**L3** and **L5**) presented quite different affinity constants [K(**L3⊂D3**) and K(**L5⊂D3**)] compared with previously studied ligands (Table 1). This confirms that longer internitrogen distances than that in **L2** are required to achieve a good fit. While ligand **L3** had an improved association constant of 1.1×10^5 M^{-1}, the longer ligand **L5** had even higher association constant (7.6×10^6 M^{-1}). It was necessary to add only 1 equiv of ligand to completely shift the Soret absorption band to 431 nm. Given this value, the estimation of the association constant for this ligand is at the limit of the fluorescence technique, but in any case, it provides an idea of the good complementarity between the ligands and **D3**. These differences could be explained because the larger ligand reaches both zinc ions within the cavity of the host. Alternatively, the existence of steric impediments between the bulky central pyrene of **L3** with the internal walls of **D3** might hamper a good interaction with the two porphyrin moieties.

Therefore, a new ligand **L4** (Scheme 4) with a similar length (15.8 Å) to that of **L3** but less sterically demanding and with

DOI: 10.1021/jacs.6b10456
J. Am. Chem. Soc. 2017, 139, 776−784

more flexibility was studied. This new ligand provided a capsule affinity (1.2×10^8 M^{-1}, Table 1) with values that are even higher than that for **L5**. The result clearly indicates that the observed low binding affinity of **L3** must be related to the size of the central ring.

Larger ligands such as **L6**, **L7**, and **L8** (Scheme 4, Figure 2SI) gave, as expected, smaller association constants (Table 1). The increment of almost 2 Å in the length of ligand **L6** compared to that of **L5** led to a reduction in the affinity for **D3** by ~5 times. This confirms that the best ligands are those with lengths between 15.8 and 16.6 Å as these fit well with the estimated capsule dimensions.

NMR Solution Studies. The self-assembling properties of CPs were characterized by ^{1}H NMR spectroscopy. In nonpolar solvents, **CP1**, **CP2**, and **CP3** form the corresponding dimers, as expected considering the previously estimated association constant for octamers.[28] These CPs, due to the C_2-symmetry, form two nonequivalent dimers that are differentiated by the amino acid interstrand pairwising, i.e., the eclipsed dimers ($\mathbf{D}_E$) and alternated dimers ($\mathbf{D}_A$) (Scheme 6 and Scheme 6SI). As a consequence, two sets of signals, particularly for amide protons, could be observed in the ^{1}H NMR spectra (Figure 4SI in Supporting Information).[13,14]

Scheme 6. Capsule Models ($\mathbf{D}_E$ and $\mathbf{D}_A$) for CP3

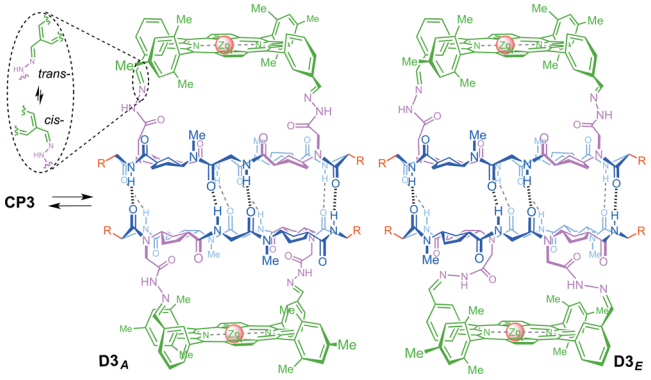

The capsule **D3** had low solubility in deuterochloroform, and the NMR spectrum showed broad signals, perhaps as a consequence of the lack of appropriate molecules that could fill the cavity of the capsule.[27] It was necessary to carry out the NMR experiments in the presence of 10% DMSO to solubilize the sample and to obtain sharp well-defined signals, see Figure 5SI. The ^{1}H NMR spectrum (Figure 2c) contained signals that can only be attributed to two nonequivalent forms (7:4 ratio) in spite of the possible existence of the two dimers ($\mathbf{D3}_E$ **and** $\mathbf{D3}_A$), together with *cis*–*trans* hydrazine geometries that increase the number of different species (Scheme 6).

Encapsulation Studies by NMR. The encapsulation processes were also studied by ^{1}H NMR spectroscopy. We started with **L5** because of its high affinity and also due to its rigidity, which reduces the potential number of different conformations. The addition of this ligand to a solution of **D3** in 10% DMSO in chloroform led to pronounced changes in the ^{1}H NMR spectra (Figure 2), such as the upfield shift and the simplification to one single peak of the signal due to the hydrazone proton. In addition, the upfield shielding of ligand proton signals [6.36 (*p*-phenylene ring), 5.55 ppm (*m*-Py), and 2.51 ppm (*o*-Py)] is characteristic of pyridine ligands sandwiched between Zn-porphyrin units.[10]

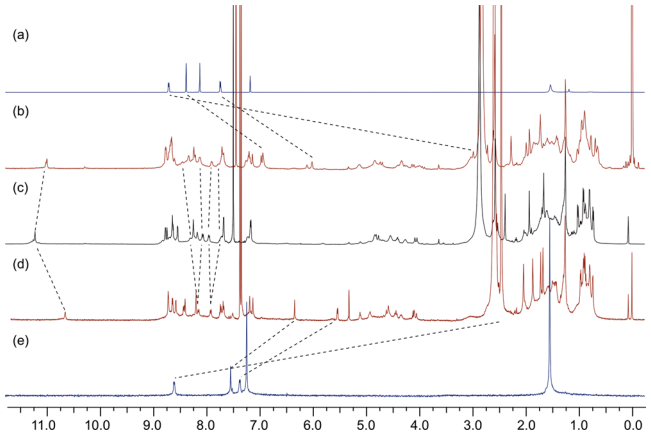

Figure 2. Selected ^{1}H NMR spectra in 10% DMSO in chloroform of **D3** (5 mM, c), with ligands **L3** (b) and **L5** (d) and ligands **L3** (a) and **L5** (e) only cyclic peptide **D3**.

The ^{1}H spectrum with ligand **L3** (Figure 2a,b) showed similar features for ligand encapsulation. The pyridine protons were also shifted upfield and resonated at 6.02, 6.12, and 2.99 ppm. In this case some of the signals appeared to be duplicated, which suggests the formation of two different complexes that interconvert slowly on the NMR time scale.

Bidimensional NMR experiments on **L3⊂D3** provided further clear evidence that **L3** is inside **D3** (Figure 3). For

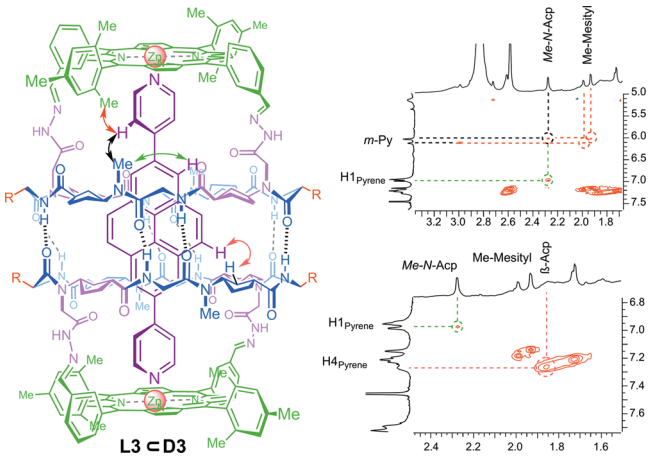

Figure 3. Selected NOESY spectra of **D3** (5 mM) in 10% DMSO/$CDCl_3$ with **L3** showing the cross peaks that confirm ligand encapsulation.

example, the clear NOE cross peaks between *m*-Py protons (at 6.12 and 6.02 ppm) and methyls of porphyrin mesitylene moieties are pointing toward the internal cavity of the dimer structure (cross peaks visible for both ligand signals) and the *N*-methyl group of Acp residues. In addition, the NOE cross peak between pyrene H1 of **L3** and the *N*-methyl group of CP is another clear indication of ligand encapsulation. Finally, the NOE for H4 of the pyrene moiety with H2 of Acp also confirms the internal disposition of **L3** in the cavity of **D3**. The existence of all of these cross peaks not only confirms ligand encapsulation but also is perhaps indicative of the strong contacts between the components, a factor that is responsible for the observed low association constant.

Diffusion ordered spectroscopy (DOSY) was carried out on samples containing **CP3** (2 mM in 10% DMSO/$CDCl_3$) and

DOI: 10.1021/jacs.6b10456
J. Am. Chem. Soc. 2017, 139, 776–784

L3 (Figure 7aSI).[28] The self-diffusion rates obtained in DOSY experiments were compared with those measured for tetrakis-(trimethylsilyl)silane (TMSS). This experiment confirmed that **L3** and capsule **D3** diffuse at the same rate. Larger aggregates were not observed, thus confirming that the Zn-pyridine interaction takes place inside the capsule and not through the external face. In this case the formation of long aggregates should be observed. The apparent hydrodynamic radius (r_H) was measured to be 14.0 ± 0.4 Å (see SI).[29] Similar results were obtained for ligand **L5** (Figure 7bSI).

Circular Dichroism (CD) Studies. The interaction of ligands **L3** and **L5** with the capsule **D3** was also monitored by CD spectroscopy (Figure 8SI).[30] Free capsule **D3** in chloroform gave rise to CD signals at 100 μM concentrations that showed a positive bisignate Cotton effect in the porphyrin Soret band, thus confirming the transfer of chirality from the peptide backbone to the porphyrin cap. The addition of the ligand (**L3** or **L5**) caused the inversion of the sign of the Cotton effect. The small bands, at 270 nm for **L3** and 340 nm for **L5**, correspond to the ligands, see UV spectra in the Supporting Information (Figure 9aSI). This can probably be ascribed to the formation of the complex, in which the conformational restrictions introduced by the two porphyrins are able to transmit the backbone chirality to the chromophores.

Thermodynamic Characterization of the Formation of Host–Guest Complexes. To carry out the thermodynamic analysis of these results, a series of equilibria can be proposed that make this system quite complex (see Schemes 4SI and 5SI in Supporting Information). Unfortunately, the signal emission for all of the proposed equilibria components must be identical as the Soret band shifts to 431 nm. As a consequence, only a qualitative evaluation of the different ligands could be made by using some simplifications.[31] The monomeric ligands **L1** can interact in solution with either **CP3** or **D3**. Depending on the face at which **L1** interacts with the monomeric form, either **CP3**·**L1** or **L1**⊂**CP3** would be formed. The latter is the intermediate responsible for ligand encapsulation to give **L1**⊂**D3**. As the first assumption, we considered that microscopic constants K_{Mi}(**L1**) (coordination with the concave face of the cavitand) and K_{M1}(**L1**) (coordination through the convex face) are almost identical on the basis of the fact that the CP diameter is large enough compared to the ligand sizes. In any case, considering the association constant of **CP3** to form **D3** [K_d(**CP3**) ~ 10^8 M^{-1}] and the concentration at which the measurements were carried out, the main component in solution must be the dimeric form.[26] As a consequence, the interactions most likely observed by UV are those between the porphyrin caps of **D3** and the ligands. The macroscopic constant for the overall process K_D(**L1**) is equal to the square of the microscopic constant K(**L1**), see eq 8 in Scheme 5SI in the SI.[32] We also assumed that there are no changes in the porphyrin properties upon the dimerization of CP to form **D3**. The affinities of ligands **L1a–c** [K_D(**L1**)] measured by UV titrations, see Table 1, were used as models for the interaction between the pyridine ligands and the porphyrin moiety, **L1a** for **L2** and **L5**, and 4-picoline (**L1b**) for **L4** and **L1c** for the rest of the ligands (**L3**, **L6**, **L7**, and **L8**). These values, although smaller, are consistent with those obtained with porphyrin **10** and others reported in the literature for similar zinc-porphyrin complexes.[23]

The stability constants for all the complexes were statistically estimated using the following equations:

$$K_{M1}(\mathbf{Ln}) = [\mathbf{Ln}\cdot\mathbf{CP3}]/([\mathbf{Ln}][\mathbf{CP3}]) \sim 2 \times K(\mathbf{L1}) \quad (1)$$

$$K_{Mi}(\mathbf{Ln}) = [\mathbf{Ln} \subset \mathbf{CP3}]/([\mathbf{Ln}][\mathbf{CP3}]) \sim K_{M1}(\mathbf{Ln}) = 2 \times K(\mathbf{L1}) \quad (2)$$

$$K_{Mi2}(\mathbf{Ln}) = [\mathbf{Ln} \subset \mathbf{D3}]/([\mathbf{Ln} \subset \mathbf{CP3}][\mathbf{CP3}]) = K_d(\mathbf{CP3}) \times K_{Mi}(\mathbf{Ln}) \times \mathrm{EM} = K_d(\mathbf{CP3}) \times 2 \times K(\mathbf{L1}) \times \mathrm{EM} \quad (3)$$

$$K(\mathbf{Ln} \subset \mathbf{D3}) = [\mathbf{Ln} \subset \mathbf{D3}]/([\mathbf{Ln}] \times [\mathbf{D3}]) = 1/K_d(\mathbf{CP3}) \times K_{Mi}(\mathbf{Ln}) \times K_{Mi2}(\mathbf{Ln}) = 4 \times [K(\mathbf{L1})]^2 \times \mathrm{EM} \quad (4)$$

$$\mathrm{EM} = K(\mathbf{Ln} \subset \mathbf{D3})/(4 \times [K(\mathbf{L1})]^2) = K(\mathbf{Ln} \subset \mathbf{D3})/(4 \times K_D(\mathbf{L1})) \quad (5)$$

The direct equilibrium between the bipyridines and the capsule was proposed to form the aforementioned **Ln**⊂**D3** through the monomeric **Ln**⊂**CP3** (Scheme 5). The formation of **Ln**⊂**D3** takes place when the trapped ligand fits in the cavity and interacts with both Zn ions. The association constants for those processes in which only one pyridine moiety interacts with the porphyrin should have twice the microscopic constant for the structurally equivalent monovalent ligands **L1**, i.e., as illustrated by eq 1, K_{M1}(**Ln**) = 2 × K(**L1**).

As mentioned for monovalent ligands, **CP3** can interact with the ligand through either of the porphyrin faces, i.e., external or internal, to form **CP3**·**Ln** (Scheme 5SI) or **Ln**⊂**CP3** (Scheme 5) complexes, respectively. The microscopic affinity constants K_{M1}(**Ln**) and K_{Mi}(**Ln**) were considered to be identical. Therefore, we deemed K_{M1}(**Ln**) ~ K_{Mi}(**Ln**), eq 2. Once **Ln**⊂**CP3** is formed, the last step [K_{Mi2}(**Ln**)] involves the combination of both the nitrogen–Zn interaction [K_{Mi}(**Ln**)] and CP dimerization [K_d(**CP3**)]. Both constants should be corrected by the effective molarity value (EM). Therefore, K_{Mi2}(**Ln**) = K_d(**CP3**) × 2 × K(**L1**) × EM (eq 3). The EM would provide quantification of the goodness of fit for our design that would only depend on the coefficient between the calculated stability constant for each ligand, K(**Ln**⊂**D3**), versus 4 times the macroscopic constant for the model pyridine ligands (K_D(**L1**)) (eq 5). The fit returned a calculated stability constant for the complex with ligand **L2** of K(**L2**⊂**D3**) = 1.1 × 10^3 M^{-1}. The application of eq 5 provided an estimated effective molarity (EM) value of 2.7 × 10^{-4} M, and this confirms the lack of complementarity of all the possible interactions.

Ligand **L3** gave an improved EM (6.0 × 10^{-3} M), but this was still far from a good fit. This value confirms the difficulties that the ligand has in entering deeply into the dimer cavity. We believe that is not related to the ligand length. In fact, ligand **L4**, which has a similar length to that of **L3**, has an EM improvement of 3 orders of magnitude (1.1 M). Although **L4** gave the largest association constant, this is not the ligand that provides the best effective molarity, which corresponds to **L5** with an EM of 1.9 M. These results suggest that the distance between the two Zn ions in the capsule is around 15.8–16.6 Å. The observed differences between these two ligands can be related to the ligand flexibility. Larger ligands provide a looser interaction with the host as a consequence of the reduction in the complementarity of the interactions between the two

DOI: 10.1021/jacs.6b10456
J. Am. Chem. Soc. 2017, 139, 776–784

fragments of the capsule and the ligand. In any case, even the larger ligand (**L8**) has a higher EM than ligands **L2** and **L3**. This finding must reflect the flexibility of the capsule to incorporate long ligands, but in contrast, the capsule might not be able to shrink to have a good fit with short ligands (**L2**).

Ligand Liberation and Equilibrium Control. Once ligand encapsulation had been confirmed, we proceeded to study its release. Several alternatives were proposed such as addition of polar protic solvents, hydrolysis of the reversible covalent linker, or competition experiments. The dilution of a 0.5 μM solution of **L*n*⊂D3** with methanol by up to 3 times (0.15 μM) did not produce significant changes in the UV−vis spectra of the complex that confirm their stability. Alternatively, the use of a 3-aminocyclohexanecarboxylic acid (Ach)-based cyclic peptide to form heterodimeric structures was also evaluated (Scheme 7).[26,33] Previous work in our group showed that Ach- and Acp-based CPs form heterodimers that are more stable than the corresponding homodimers.

Scheme 7. Competition Experiments between Complementary Cyclic Peptides CP3 and CP4 and Ligand L5

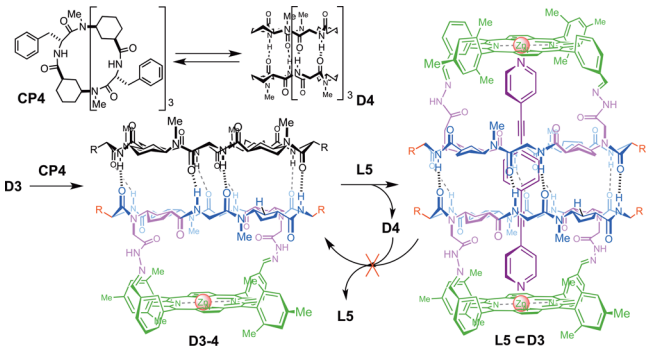

The addition of 1 equiv of (Ach)-based **CP4** gave the heterodimeric cavitand **D3-4**, as confirmed by NMR experiments in which a new set of signals appeared (Scheme 7 and Figure 10SI). The addition of bidentate ligands such as **L5** gave rise to changes in the chemical shifts to give an NMR spectrum that was similar to that of the previously prepared complex **L5⊂D3** (Figure 11SI). The NH chemical shifts (8.17 and 7.94 ppm) together with the typical signals of the encapsulated guests provide clear evidence for the formation of the proposed structure. UV experiments also confirmed the formation of **L5⊂D3**, with the Soret band shifted to 431 nm on addition of 1 equiv of ligand. On the other hand, the addition of up to almost 600 equiv of **CP4** to a 1 μM solution of **L5⊂D3** in chloroform did not give any change in the UV spectrum (Figure 12SI), thus confirming the strength of the host−guest complex and the inability to liberate the ligand by this approach.

Finally, hydrolysis of the hydrazone linkage was the most successful alternative to liberate the encapsulated ligand (Scheme 8). The addition of *O*-benzylhydroxylamine in 10% DMSO in chloroform to a solution containing **L5⊂D3** led to liberation of ligand **L5** upon separation of the porphyrin and CP components. The process was studied by UV−vis spectroscopy, following the disappearance of the 431 nm Soret band with time (Figure 13aSI). A total of 20 h was required to observe the complete shift of the Soret band from 431 to 421 nm (Figure 13bSI). This confirmed the liberation of **L5** into the solution.

Scheme 8. Simplified Model for Ligand Liberation by Hydrolysis of Hydrazone Linker

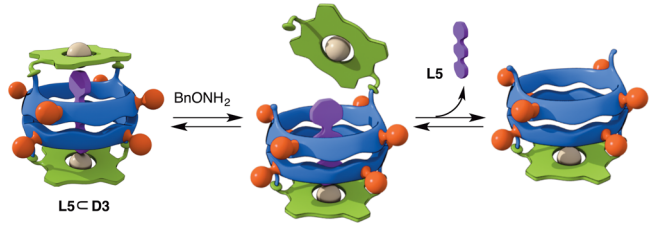

CONCLUSIONS

A new supramolecular capsule has been designed that is a dimer of α,γ-CPs bearing Zn-porphyrin caps. The self-assembled dimer can recognize and encapsulate bipyridine-based ligands of suitable size. The proposed design combines dynamic covalent bonds for the preparation of the hemicapsule (cavitand), hydrogen bonding interactions for peptide self-dimerization and capsule formation, and metal coordination for ligand recognition. The complexation of the self-assembled bisporphyrin receptor **D3** with ditopic ligands was studied by performing UV−vis, ^{1}H NMR, and CD experiments. The designed ligands allow a precise determination of the length of the **D3** cavity. The best ligands, i.e., those with higher EM values, are those with an internitrogen separation between 15.8 and 16.6 Å. The encapsulated ligands can be liberated by using the reversibility of the hydrazone connection. Formation of an oxime bond between the porphyrin cap and *o*-benzylhydroxylamine hydrolyzed the linker to liberate the entrapped ligand. The proposed design, in which a porphyrin cap is combined with a cyclic peptide, has significant advantages such as allowing the modification of internal cavity properties without altering the self-assembling properties of the peptide capsule.[34]

We envisage that, after some structural redesign, these capsules might find applications in drug delivery vehicles, molecular machines, nanoreactors, sensors, or light-induced energy- and electron-transfer switches regulated by bipyridine coordination. Such systems would require the introduction of additional chromophores into the cyclic peptide scaffold.

ASSOCIATED CONTENT

Supporting Information

The Supporting Information is available free of charge on the ACS Publications website at DOI: 10.1021/jacs.6b10456.

Synthetic procedures, further schemes and figures, and NMR and MS data (PDF)

AUTHOR INFORMATION

Corresponding Author

*juanr.granja@usc.es

ORCID

Juan R. Granja: 0000-0002-5842-7504

Notes

The authors declare no competing financial interest.

ACKNOWLEDGMENTS

H.L.O. thanks Mineco for his FPU contract and the Diputación de A Coruña for his research fellowship. We also thank the ORFEO-CINCA network. This work was supported by the Spanish Ministry of Economy and Competitivity (Mineco) and the ERDF (CTQ2013-43264-R and CTQ2014-51912-REDC),

DOI: 10.1021/jacs.6b10456
J. Am. Chem. Soc. 2017, 139, 776−784

and by the Xunta de Galicia and the ERDF (EM2014/011 and Centro singular de investigación de Galicia accreditation 2016-2019, ED431G/09).

REFERENCES

(1) (a) Ballester, P.; Fujita, M.; Rebek, J. *Chem. Soc. Rev.* **2015**, *44*, 392−393. (b) Zarra, S.; Wood, D. M.; Roberts, D. A.; Nitschke, J. R. *Chem. Soc. Rev.* **2015**, *44*, 419−432. (c) Dariush, A. Self-assembled molecular capsule. In *Synergy in Supramolecular Chemistry*; Tatsuya, N., Ed.; CRC Press: Boca Raton, FL, 2015; pp 133−148. (d) Smulders, M. M. J.; Riddell, I. A.; Browne, C.; Nitschke, J. R. *Chem. Soc. Rev.* **2013**, *42*, 1728−1754. (e) Chakrabarty, R.; Mukherjee, P. S.; Stang, P. J. *Chem. Rev.* **2011**, *111*, 6810−6918. (f) Forgan, R. S.; Sauvage, J.-P.; Stoddart, J. F. *Chem. Rev.* **2011**, *111*, 5434−5464. (g) Saalfrank, R. W.; Maid, H.; Scheurer, A. *Angew. Chem., Int. Ed.* **2008**, *47*, 8794−8824. (h) Conn, M. M.; Rebek, J. *Chem. Rev.* **1997**, *97*, 1647−1668.

(2) Yoshizawa, M.; Klosterman, J. K.; Fujita, M. *Angew. Chem., Int. Ed.* **2009**, *48*, 3418−3438.

(3) (a) Natarajan, A.; Kaanumalle, L. S.; Jockusch, S.; Gibb, C. L. D.; Gibb, B. C.; Turro, N. J.; Ramamurthy, V. *J. Am. Chem. Soc.* **2007**, *129*, 4132−4133. (b) Cullen, W.; Misuraca, M. C.; Hunter, C. A.; Williams, N. H.; Ward, M. D. *Nat. Chem.* **2016**, *8*, 231−236.

(4) (a) Cram, D. J.; Karbach, S.; Kim, Y. H.; Baczynskyj, L.; Kallemeyn, G. W. *J. Am. Chem. Soc.* **1985**, *107*, 2575−2576. (b) Canceill, J.; Cesario, M.; Collet, A.; Guilhem, J.; Pascard, C. *J. Chem. Soc., Chem. Commun.* **1985**, *6*, 361−363. (c) Liu, F.; Helgeson, R. C.; Houk, K. N. *Acc. Chem. Res.* **2014**, *47*, 2168−2176.

(5) (a) Wyler, R.; de Mendoza, J.; Rebek, J., Jr *Angew. Chem., Int. Ed. Engl.* **1993**, *32*, 1699−1701. (b) Meissner, R.; Rebek, J., Jr.; de Mendoza, J. *Science* **1995**, *270*, 1485−1488. (c) Ajami, D.; Rebek, J., Jr. *Acc. Chem. Res.* **2013**, *46*, 990−999.

(6) (a) Brown, F. D.; Toste, R. G.; Bergman, R. G.; Raymond, K. N. *Chem. Rev.* **2015**, *115*, 3012−3035. (b) Cook, T. R.; Zheng, Y.-R.; Stang, P. J. *Chem. Rev.* **2013**, *113*, 734−777.

(7) (a) Harris, K.; Fujita, D.; Fujita, M. *Chem. Commun.* **2013**, *49*, 6703−6712. (b) Liu, Y.; Hu, C.; Comotti, A.; Ward, M. D. *Science* **2011**, *333*, 436−440. (c) Fujita, D.; Ueda, Y.; Sato, S.; Yokoyama, H.; Mizuno, N.; Kumasaka, T.; Fujita, M. *Chem.* **2016**, *1*, 91−101.

(8) (a) Catti, L.; Zhang, Q.; Tiefenbacher, K. *Chem. - Eur. J.* **2016**, *22*, 9060−9066. (b) Schmidt, B. M.; Osuga, T.; Sawada, T.; Hoshino, M.; Fujita, M. *Angew. Chem., Int. Ed.* **2016**, *55*, 1561−1564. (c) Wang, Q.-Q.; Gonell, S.; Leenders, S. H. A. M.; Dürr, M.; Ivanović-Burmazović, I.; Reek, J. N. H. *Nat. Chem.* **2016**, *8*, 225−230. (d) Jansze, S. M.; Cecot, G.; Wise, M. D.; Zhurov, K. O.; Ronson, T. K.; Castilla, A. M.; Finelli, A.; Pattison, P.; Solari, E.; Scopelliti, R.; Zelinskii, G. E.; Vologzhanina, A. V.; Voloshin, Y. Z.; Nitschke, J. R.; Severin, K. *J. Am. Chem. Soc.* **2016**, *138*, 2046−2054. (e) Korom, S.; Martin, E.; Serapian, S. A.; Bo, C.; Ballester, P. *J. Am. Chem. Soc.* **2016**, *138*, 2273−2279. (f) Chen, S.; Li, K.; Zhao, F.; Zhang, L.; Pan, M.; Fan, Y.-Z.; Guo, J.; Shi, J.; Su, C.-Y. A *Nat. Commun.* **2016**, *7*, 13169. (g) Catti, L.; Zhang, Q.; Tiefenbacher, K. *Synthesis* **2016**, *48*, 313−328. (h) Catti, L.; Zhang, Q.; Tiefenbacher, K. *Chem. - Eur. J.* **2016**, *22*, 9060−9066. (i) Kaphan, D. M.; Levin, M. D.; Bergman, R. G.; Raymond, K. N.; Toste, F. D. *Science* **2015**, *350*, 1235−1238. (j) Leenders, S. H. A. M.; Gramage-Doria, R.; de Bruin, B.; Reek, J. N. H. *Chem. Soc. Rev.* **2015**, *44*, 433−448. (k) Ramamurthy, V. *Acc. Chem. Res.* **2015**, *48*, 2904−2917. (l) Andrade, B.; Song, Z.; Li, J.; Zimmerman, S. C.; Cheng, J.; Moore, J. S.; Harris, K.; Katz, J. S. *ACS Appl. Mater. Interfaces* **2015**, *7*, 6359−6368. (m) Castilla, A. M.; Ramsay, W. J.; Nitschke, J. R. *Acc. Chem. Res.* **2014**, *47*, 2063−2073. (n) Ramamurthy, V.; Gupta, S. *Chem. Soc. Rev.* **2015**, *44*, 119−135. (o) Dutta, R.; Ghosh, P. *Chem. Commun.* **2014**, *50*, 10538−10554. (p) Yamanaka, M.; Kawaharada, M.; Nito, Y.; Takaya, H.; Kobayashi, K. *J. Am. Chem. Soc.* **2011**, *133*, 16650−16656. (q) Mugridge, J. S.; Szigethy, G.; Bergman, R. G.; Raymond, K. N. *J. Am. Chem. Soc.* **2010**, *132*, 16256−16264.

(9) (a) Galán, A.; Ballester, P. *Chem. Soc. Rev.* **2016**, *45*, 1720−1737. (b) Helttunen, K.; Galán, A.; Ballester, P.; Bergenholtz, J.; Nissinen, M. *J. Colloid Interface Sci.* **2016**, *464*, 59−65. (c) Ballester, P.; Gil-Ramírez, G. *Proc. Natl. Acad. Sci. U. S. A.* **2009**, *106*, 10455−10459. (d) Custelcean, R. *Chem. Commun.* **2013**, *49*, 2173. (e) Amouri, H.; Desmarets, C.; Moussa, J. *Chem. Rev.* **2012**, *112*, 2015−2041.

(10) (a) Durot, S.; Taesch, J.; Heitz, V. *Chem. Rev.* **2014**, *114*, 8542−8578. (b) Meng, W.; Breiner, B.; Rissanen, K.; Thoburn, J. D.; Clegg, J. K.; Nitschke, J. R. *Angew. Chem., Int. Ed.* **2011**, *50*, 3479−3483. (c) Otte, M.; Kuijpers, P. F.; Troeppner, O.; Ivanovic-Burmazovic, I.; Reek, J. N. H.; de Bruin, B. *Chem. - Eur. J.* **2013**, *19*, 10170−10178. (d) Shi, Y. H.; Sánchez-Molina, I.; Cao, C. S.; Cook, T. R.; Stang, P. J. *Proc. Natl. Acad. Sci. U. S. A.* **2014**, *111*, 9390−9395. (e) D'Urso, A.; Fragala, M. E.; Purrello, R. *Chem. Commun.* **2013**, *49*, 4441−4443. (f) Boccalon, M.; Iengo, E.; Tecilla, P. *Org. Biomol. Chem.* **2013**, *11*, 4056−4067. (g) Samanta, S. K.; Schmittel, M. *J. Am. Chem. Soc.* **2013**, *135*, 18794−18797. (h) Hoffmann, M.; Kärnbratt, J.; Chang, M.-H.; Herz, L. M.; Albinsson, B.; Anderson, H. L. *Angew. Chem., Int. Ed.* **2008**, *47*, 4993−4996. (i) Lifschitz, A. M.; Rosen, M. S.; McGuirk, C. M.; Mirkin, C. A. *J. Am. Chem. Soc.* **2015**, *137*, 7252−7261.

(11) (a) Kishimoto, K.; Nakamura, M.; Kobayashi, K. *Chem. - Eur. J.* **2016**, *22*, 2629−2633. (b) Wood, D. M.; Meng, W.; Ronson, T. K.; Stefankiewicz, A. R.; Sanders, J. K. M.; Nitschke, J. R. *Angew. Chem., Int. Ed.* **2015**, *54*, 3988−3992. (c) Nakazawa, J.; Mizuki, M.; Shimazaki, Y.; Tani, F.; Naruta, Y. *Org. Lett.* **2006**, *8*, 4275−4278. (d) Ikeda, A.; Ayabe, M.; Shinkai, S.; Sakamoto, S.; Yamaguchi, K. A. *Org. Lett.* **2000**, *2*, 3707−3710.

(12) (a) Bong, D. T.; Clark, T. D.; Granja, J. R.; Ghadiri, M. R. *Angew. Chem., Int. Ed.* **2001**, *40*, 988−1011. (b) Brea, R. J.; Reiriz, C.; Granja, J. R. *Chem. Soc. Rev.* **2010**, *39*, 1448−1456. (c) Chapman, R.; Danial, M.; Koh, M. L.; Jolliffe, K. A.; Perrier, S. *Chem. Soc. Rev.* **2012**, *41*, 6023−6041.

(13) (a) Amorín, M.; Castedo, L.; Granja, J. R. *J. Am. Chem. Soc.* **2003**, *125*, 2844−2845. (b) Brea, R. J.; Castedo, L.; Granja, J. R. *Chem. Commun.* **2007**, 3267−3269. (c) Amorín, M.; Castedo, L.; Granja, J. R. *Chem. - Eur. J.* **2005**, *11*, 6543−6551. (d) Ghadiri, M. R.; Kobayashi, K.; Granja, J. R.; Chadha, R. K.; McRee, D. E. *Angew. Chem., Int. Ed. Engl.* **1995**, *34*, 93−95.

(14) (a) Reiriz, C.; Amorín, M.; García-Fandiño, R.; Castedo, L.; Granja, J. R. *Org. Biomol. Chem.* **2009**, *7*, 4358−4361. (b) Rodríguez-Vázquez, N.; García-Fandiño, R.; Amorín, M.; Granja, J. R. *Chem. Sci.* **2016**, *7*, 183−187.

(15) Sanchez-Quesada, J.; Isler, M. P.; Ghadiri, M. R. *J. Am. Chem. Soc.* **2002**, *124*, 10004−10005.

(16) (a) Rodríguez-Vázquez, N.; Salzinger, S.; Silva, L. F.; Amorín, M.; Granja, J. R. *Eur. J. Org. Chem.* **2013**, *2013*, 3477−3493. (b) Reiriz, C.; Castedo, L.; Granja, J. R. *J. Pept. Sci.* **2008**, *14*, 241−249.

(17) For previous studies in the design of CP-porphyrin tweezers, see: (a) Hernández-Eguía, L. P.; Brea, R. J.; Castedo, L.; Ballester, P.; Granja, J. R. *Chem. - Eur. J.* **2011**, *17*, 1220−1229. (b) Aragay, G.; Ventura, B.; Guerra, A.; Pintre, I.; Chiorboli, C.; García-Fandiño, R.; Flamigni, L.; Granja, J. R.; Ballester, P. *Chem. - Eur. J.* **2014**, *20*, 3427−3438.

(18) (a) Littler, B. J.; Ciringh, Y.; Lindsey, J. S. *J. Org. Chem.* **1999**, *64*, 2864−2872. (b) Lee, C. H.; Lindsey, J. S. *Tetrahedron* **1994**, *50*, 11427−11440.

(19) (a) Fukuyama, T.; Jow, C. K.; Cheung, M. *Tetrahedron Lett.* **1995**, *36*, 6373−6374. (b) Fukuyama, T.; Cheung, M.; Jow, C. K.; Hidai, Y.; Kan, T. *Tetrahedron Lett.* **1997**, *38*, 5831−5834.

(20) Isidro-Llobet, A.; Álvarez, M.; Albericio, F. *Chem. Rev.* **2009**, *109*, 2455−2504.

(21) *DynaFit, version 4.07*; BioKin Ltd.

(22) (a) Kuzmič, P. *Anal. Biochem.* **1996**, *237*, 260−273. (b) Kuzmič, P. *Methods Enzymol.* **2009**, *467*, 247−280.

(23) (a) Summers, J. S.; Stolzenberg, A. M. *J. Am. Chem. Soc.* **1993**, *115*, 10559−10567. (b) Cole, S. J.; Curthoys, G. C.; Magnusson, E. A.; Phillips, J. N. *Inorg. Chem.* **1972**, *11*, 1024−1028. (c) Satake, A.; Kobuke, Y. *Tetrahedron* **2005**, *61*, 13−41.

(24) Hunter, C. A.; Sanders, J. K.; Stone, A. J. *Chem. Phys.* **1989**, *133*, 395−404.

(25) (a) Hermann, K.; Ruan, Y.; Hardin, A. M.; Hadad, C. M.; Badjic, J. D. *Chem. Soc. Rev.* **2015**, *44*, 500−514. (b) Santamaría, J.; Martín, T.;

DOI: 10.1021/jacs.6b10456
J. Am. Chem. Soc. 2017, 139, 776−784

Hilmersson, G.; Craig, S. L.; Rebek, J., Jr. *Proc. Natl. Acad. Sci. U. S. A.* **1999**, *96*, 8344−8347.
(26) Brea, R. J.; Pérez-Alvite, M. J.; Panciera, M.; Mosquera, M.; Castedo, L.; Granja, J. R. *Chem. - Asian J.* **2011**, *6*, 110−121.
(27) Mecozzi, S.; Rebek, J., Jr. *Chem. - Eur. J.* **1998**, *4*, 1016−1022.
(28) Avram, L.; Cohen, Y. *Chem. Soc. Rev.* **2015**, *44*, 586−602.
(29) (a) Macchioni, A.; Ciancaleoni, G.; Zuccaccia, C.; Zuccaccia, D. *Chem. Soc. Rev.* **2008**, *37*, 479−489. (b) Zuccaccia, D.; Macchioni, A. *Organometallics* **2005**, *24*, 3476−3486.
(30) Gottarelli, G.; Lena, S.; Masiero, S.; Pieraccini, S.; Spada, G. P. *Chirality* **2008**, *20*, 471−485.
(31) For a more detailed explanation about the equilibrium processes, see Supporting Information (page 7SI).
(32) Martinez, J. C.; Murciano-Calles, J.; Cobos, E. S.; Iglesias-Bexiga, M.; Luque, M. I.; Ruiz-Sanz, J. Isothermal Titration Calorimetry: Thermodynamic Analysis of the Binding Thermograms of Molecular Recognition Events by Using Equilibrium Models. In *Applications of Calorimetry in a Wide Context—Differential Scanning Calorimetry, Isothermal Titration Calorimetry and Microcalorimetry*; Elkordy, A. A., Ed.; InTech: Rijeka, Croatia, 2013; Chapter 4.
(33) Brea, R. J.; Amorín, M.; Castedo, L.; Granja, J. R. *Angew. Chem., Int. Ed.* **2005**, *44*, 5710−5713.
(34) Adriaenssens, L.; Ballester, P. *Chem. Soc. Rev.* **2013**, *42*, 3261−3277.

DOI: 10.1021/jacs.6b10456
J. Am. Chem. Soc. 2017, 139, 776−784